Journal of Neurochemistry

JOURNAL OF NEUROCHEMISTRY | 2009 | 109 | 1800–1811 doi: 10.1111/j.1471-4159.2009.06107.x

Distinct modulation of voltage-gated and ligand-gated Ca^{2+} currents by PPAR-γ agonists in cultured hippocampal neurons

Tristano Pancani, Jeremiah T. Phelps, James L. Searcy, Michael W. Kilgore, Kuey-Chu Chen, Nada M. Porter and Olivier Thibault

Department of Molecular and Biomedical Pharmacology, University of Kentucky Medical Center, 800 Rose Street, MS 310, Lexington, Kentucky 40536-0298, USA

Abstract

Type 2 diabetes mellitus is a metabolic disorder characterized by hyperglycemia and is especially prevalent in the elderly. Because aging is a risk factor for type 2 diabetes mellitus, and insulin resistance may contribute to the pathogenesis of Alzheimer's disease (AD), anti-diabetic agents (thiazolidinediones-TZDs) are being studied for the treatment of cognitive decline associated with AD. These agents normalize insulin sensitivity in the periphery and can improve cognition and verbal memory in AD patients. Based on evidence that Ca^{2+} dysregulation is a pathogenic factor of brain aging/AD, we tested the hypothesis that TZDs could impact Ca^{2+} signaling/homeostasis in neurons. We assessed the effects of pioglitazone and rosiglitazone (TZDs) on two major sources of Ca^{2+} influx in primary hippocampal cultured neurons, voltage-gated Ca^{2+} channel (VGCC) and the NMDA receptor (NMDAR). VGCC- and NMDAR-mediated Ca^{2+} currents were recorded using patch-clamp techniques, and Ca^{2+} intracellular levels were monitored with Ca^{2+} imaging techniques. Rosiglitazone, but not pioglitazone reduced VGCC currents. In contrast, NMDAR-mediated currents were significantly reduced by pioglitazone but not rosiglitazone. These results show that TZDs modulate Ca^{2+}-dependent pathways in the brain and have different inhibitory profiles on two major Ca^{2+} sources, potentially conferring neuroprotection to an area of the brain that is particularly vulnerable to the effects of aging and/or AD.

Keywords: aging, Alzheimer's disease, Ca^{2+} signaling, diabetes, electrophysiology, neuroprotection.

J. Neurochem. (2009) **109**, 1800–1811.

Several studies have reported that similar neuropathological mechanisms are present in aging and/or Alzheimer's disease (AD) and in diabetes mellitus. An increased risk of dementia (Alzheimer's and vascular type) is seen in people with diabetes (Ott *et al.* 1999; Schnaider Beeri *et al.* 2004; Biessels *et al.* 2006), and aging is a recognized risk factor for both AD and diabetes (Hoyer 2004; Yaffe *et al.* 2004; Launer 2005; McNay 2005; Reagan 2007). Furthermore, insulin resistance associated with type 2 diabetes mellitus (T2DM) may be an important pathogenic factor in AD (Watson and Craft 2003; Steen *et al.* 2005; Li and Holscher 2007), and thought to be present in 80% of the AD population (Janson *et al.* 2004). It has been suggested that cognitive dysfunction in older adults and AD patients might reflect a CNS state of diabetes characterized by reduced insulin signaling and/or resistance, and termed 'Type 3 diabetes' (Lannert and Hoyer 1998; Gasparini *et al.* 2002; Steen *et al.* 2005; de la Monte *et al.* 2006). In older T2DM adults, cognitive dysfunction is associated with poor control of diabetes (Munshi *et al.* 2006), and improving glycemic control leads to improved cognition and memory (Ryan *et al.* 2006). Therefore, it appears that common underlying mechanisms coexist in T2DM, aging and/or AD.

Peroxisome proliferator-activated receptor (PPAR)-γ is a nuclear receptor that is a target of thiazolidinediones (TZDs) and regulates the expression of genes controlling inflammation, metabolism, cell growth, and differentiation (Berger and Moller 2002; Hauner 2002). PPAR subtypes (α, β, and γ) are present in almost all cells, including adipocytes, fibroblasts,

Received March 25, 2009; accepted April 11, 2009.

Address correspondence and reprint requests to Olivier Thibault, Department of Molecular and Biomedical Pharmacology, University of Kentucky Medical Center, 800 Rose street, MS310, Lexington, KY 40536-0298, USA. E-mail:othibau@uky.edu

Abbreviations used: AD, Alzheimer's disease; DIV, days *in vitro*; DMSO, dimethylsulfoxide; NMDAR, NMDA receptor; PIO, pioglitazone; PPAR, peroxisomal proliferator-activated receptor; PPRE, peroxisome proliferator response element; ROSI, rosiglitazone; T2DM, type 2 diabetes mellitus; TEA, tetraethylammonium; TIO, T0070907; TZD, thiazolidinedione; VGCC, voltage-gated Ca^{2+} channel.

macrophages, microglia, and neurons (Berger and Moller 2002; Hauner 2002; Cimini *et al.* 2005; Inestrosa *et al.* 2005). TZDs' mechanisms of action and biological effects are cell-type specific (Berger *et al.* 2005) and are also dependent on the structural makeup of the ligand (Nolte *et al.* 1998; Rangwala and Lazar 2002; Zhang *et al.* 2007; Gani and Sylte 2008). In adipocytes, TZDs promote lipid accumulation by increasing gene transcription for several fatty acid binding proteins (Schoonjans *et al.* 1996; Martin *et al.* 1997; Berger and Moller 2002). TZDs also appear capable of reestablishing insulin sensitivity in fat, muscle, and liver tissues, by decreasing plasma free fatty acids, lipid levels (Berger *et al.* 2005), and inflammation (Hofmann *et al.* 1994).

In a preliminary study, TZD treatment with rosiglitazone during early stages of AD has been shown to improve cognition (Watson *et al.* 2005). Testing the effects of rosiglitazone using the AD assessment scale (ADAS-Cog) in a larger population of AD patients has revealed that patients lacking the APOE4 allele appear selectively protected by the TZD (Risner *et al.* 2006). Several studies have focused on the mechanisms of action and functional role of TZDs in the brain (Feinstein 2003; Sundararajan *et al.* 2006; Jiang *et al.* 2008; Lichtor *et al.* 2008). In models of AD and neurodegeneration, mechanisms identified include decreased inflammation (Combs *et al.* 2000; Heneka *et al.* 2000, 2005; Daynes and Jones 2002; Garcia-Bueno *et al.* 2005; Hunter *et al.* 2007; Xing *et al.* 2008), decreased oxidative stress (Aoun *et al.* 2003; Garcia-Bueno *et al.* 2005; Kumar *et al.* 2009), decreased Aβ load (Combs *et al.* 2000; Yan *et al.* 2003; Camacho *et al.* 2004; Heneka *et al.* 2005; Jiang *et al.* 2008), improved mitochondrial function/number (Dello Russo *et al.* 2003; Feinstein *et al.* 2005; Fuenzalida *et al.* 2007; Strum *et al.* 2007; Hunter *et al.* 2008), and increased glial glutamate uptake (Romera *et al.* 2007).

Despite evidence that TZDs are neuroprotective, few studies have considered the impact of PPAR-γ agonists on neuronal Ca^{2+} homeostasis. This is surprising given the degree of neuronal Ca^{2+} dysregulation present in aging/AD, and the evidence that in animal models of diabetes, alterations in Ca^{2+} signaling are seen. In the streptozotocin model of diabetes, increased cytosolic and mitochondrial Ca^{2+} (Huang *et al.* 2002, 2005), larger Ca^{2+} action potentials and Ca^{2+}-dependent afterhyperpolarization, and reduced intracellular Ca^{2+} release (Huang *et al.* 2002; Kamal *et al.* 2003; Kruglikov *et al.* 2004) are seen. Further, in this model, alterations in the NMDA receptor (NMDAR) complex are thought to mediate deficits in learning and memory (Biessels *et al.* 1998; Li and Wei 2001; Gardoni *et al.* 2002). Recent evidence also shows the PPAR-γ agonist pioglitazone attenuates memory impairment in the intracerebral streptozotocin model (Pathan *et al.* 2006). Here, therefore, we tested the hypothesis that pioglitazone and rosiglitazone could reduce signaling through two aging-sensitive neuronal Ca^{2+} targets, the voltage-gated Ca^{2+} channel (VGCC) and NMDAR. Because Ca^{2+} dysregulation is a hallmark of brain aging that is linked to cognitive decline (Disterhoft *et al.* 1996; Thibault and Landfield 1996; Moyer *et al.* 2000; Tombaugh *et al.* 2005; Murphy *et al.* 2006), re-establishment of Ca^{2+} homeostasis with PPAR-γ agonists might represent a mechanism by which these compounds improve cognition with aging/AD.

Materials and methods

Cell cultures

Mixed (neuron/glia) hippocampal cultures were established from pregnant Sprague-Dawley rats as previously described (Porter *et al.* 1997). Briefly, hippocampi from E18 fetuses were removed and treated with trypsin 0.25% in Hank's balanced salt solution for 10 min. The cell suspension was triturated, diluted with minimum essential medium at a final concentration of 5×10^5 cells/mL, and added to 35 mm culture dishes. For electrophysiological experiments, the 35 mm culture dish contained three plastic coverslips (Corning Inc., Corning, NY, USA). For Ca^{2+} imaging experiments 35 mm glass bottom culture dishes were used (Mattek Corp., Ashland MA, USA). All dishes were coated with poly-L-lysine, and were maintained in an incubator until used at 13–16 days *in vitro* (DIV). For PPAR-γ binding and western blot assays, six-well plates (35 mm/well; Corning) coated with poly-L-lysine were used. Approximately 1×10^6 cells were plated in each well and used at 13–16 DIV. Solutions and media were obtained from Invitrogen Corp. (Carlsbad, CA, USA).

PPAR-γ binding assay

Quantitative measurement of PPAR-γ activation was achieved using an ELISA-based assay (TransAM kit; Active Motif, Carlsbad, CA, USA). The assay was performed according to the manufacturer's protocol. Signals were normalized to vehicle-treated cells [dimethylsulfoxide (DMSO)] and were background corrected. In brief, cells from at least three 35 mm dishes were harvested for each treatment group and processed to obtain a purified nuclear extract. The TransAM kit was supplied with a 96 well plate containing the peroxisome proliferator response element (PPRE) sequence bound at the bottom of each well, the primary antibody against the activated form of PPAR-γ and the secondary antibody (horseradish peroxidase conjugated). The nuclear extract was added to each well to let the activated PPAR-γ bind specifically to the bound oligonucleotide. After washing, the sample was incubated with the primary antibody and then with the secondary antibody. Quantification of the PPRE-bound PPAR-γ colorimetric reaction was obtained using a HTS7000+ plate reader (PerkinElmer, Waltham, MA, USA).

Western blots

The nuclear fraction from at least six 35 mm dishes per condition was isolated as above for the PPAR-γ binding assay. Total protein content was evaluated using a Bradford assay and results were used to load the same amount of protein per lane on a 10% Tris-HCl gel (Bio-Rad, Hercules, CA, USA). After electrophoresis, proteins were transferred to a nitrocellulose membrane and then incubated overnight at 4°C with the primary antibody against the N-terminus fragment of PPAR-γ 1 : 1000 (Santa Cruz Biotechnologies, Santa Cruz, CA, USA). The membrane was then incubated for 1 h with the secondary antibody, horseradish peroxidase-conjugated 1 : 5000

(Santa Cruz), and developed after treatment with ECL plus. The membrane was exposed to a radiographic film (ISCBioExpress, Kaysville, UT, USA), and imaged/quantified on a Gel Logic 2200 Imaging System (Kodak Inc., Rochester, NY, USA). The same procedure was used for β-actin immunostaining. Signal intensities for each lane was normalized to β-actin signal for that lane.

Electrophysiology and Ca^{2+} imaging

VGCC recording solutions

The extracellular solution was as follows (in mM): 111 NaCl, 5 $BaCl_2$, 5 CsCl, 2 $MgCl_2$, 10 Glucose, 10 HEPES, 20 tetraethylammonium (TEA)-Cl, pH 7.35 with NaOH. Tetrodotoxin (500 nM) was added before recording. Intracellular pipette solution was (in mM): 145 methanesulfonic acid, 10 HEPES, 3 $MgCl_2$, 11 EGTA, 1 $CaCl_2$, 13 TEA-Cl, 14 phosphocreatine Tris-salt, 4 Tris-ATP, 0.3 Tris-GTP, pH 7.3 with CsOH.

NMDAR recording solutions

The extracellular solution was as follows (in mM): 145 NaCl, 2.5 KCl, 10 HEPES, 10 Glucose, 2 $CaCl_2$, 10 TEA-Cl, pH 7.35 with NaOH. Glycine (10 μM), tetrodotoxin (500 nM), and 6-cyano-7-nitroquinoxaline-2,3-dione (10 μM) were added immediately prior to recording. Intracellular pipette solution was (in mM): 145 methanesulfonic acid, 10 HEPES, 11 EGTA, 1 $CaCl_2$, 14 phosphocreatine Tris-salt, 4 Tris-ATP, 0.3 Tris-GTP, pH 7.3 with CsOH.

Ca^{2+} imaging solutions

Bath solution contained (in mM): 145 NaCl, 2.5 KCl, 10 HEPES, 10 D-glucose, 2 $CaCl_2$, 1 $MgCl_2$, 0.01 glycine, pH 7.3 with NaOH.

Whole-cell recording

Electrodes were made from glass capillary tubes (Drummond Scientific, Broomall, PA, USA) using a P-87 micropipette puller (Sutter Instruments, Novato, CA, USA), coated with polystyrene Q-dope (GC Electronics, Rockford, IL, USA) and fire polished before recording. A coverslip was taken from the incubator, rinsed twice with recording solution and placed in the recording chamber containing 2 mL of the extracellular solution. The recording chamber was then fixed on the stage of an E600FN microscope (Nikon Inc. Melville, NY, USA). An Axopatch-1D amplifier (Molecular Devices, Sunnyvale, CA, USA) and a Digidata 1200 (Molecular Devices) were used in combination with pClamp7 (Molecular Devices) to control membrane voltage and to acquire current records (5–10 KHz). Tip resistance was 3.2 ± 0.7 MΩ. Junction potential was nulled prior to each experiment and pipette capacitance was compensated. Once whole cell configuration was achieved, a 5–10 min run-up period was allowed prior to recording of currents. Data were lowpass filtered at 2–5 kHz. For VGCC recording, an *I/V* relationship was conducted (from −60 to +30 mV, 150 ms step) to identify the voltage step corresponding to the largest current. Each cell was then held at −70 mV or −40 mV and currents were recorded in response to a step depolarization (150 or 350 ms, respectively) eliciting the largest current (as determined from the *I/V*). For each cell, leak subtraction was accomplished online using a fractional method (5–8 scaled hyperpolarizing sub-pulses). Series resistance compensation was not routinely performed since we have found that at these current amplitudes, compensation (~80%) has minimal impact (Porter *et al.* 1997). For NMDA-mediated current recording, cells were held at −70 mV and the current elicited by exposure to NMDA was monitored (see drug delivery below). All experiments were performed at room temperature (22–24°C). Because cell size contributes to current amplitude, all currents were normalized to cell capacitance (pF) and are reported as current density measures (pA/pF). Membrane capacitance was derived from the integral of the capacitative transient evoked by a 150 ms/10 mV hyperpolarizing pulse from −70 mV (Porter *et al.* 1997). For each cell, input resistance was determined from the steady current necessary to hyperpolarize the cell by 10 mV.

Ca^{2+} imaging

Glass pieces from broken 35 mm glass bottom dishes containing hippocampal cells were incubated for 30 min in the dark, in the Ca^{2+} imaging solution supplemented with 2 μM final Fura-2 AM, 0.085% final DMSO, and 0.015% final Pluronic F127 (Molecular Probes, Invitrogen). Following a 20 min deesterification period in indicator-free imaging solution, glass fragments were transferred to an imaging chamber (glass-bottom 35 mm dish) on the stage of an E600FN microscope (Nikon Inc.). Excitation of the fluorophore (340 and 380 nm excitation) was achieved using a high speed filter changer (Lambda DG4, Sutter instruments), and an Andor iXon EMCCD camera (Andor Technology, Belfast, Ireland) was used to capture emitted light (510 nm). Data acquisition and analysis were performed using Imaging Workbench 5.0 (Indec BioSystems, Santa Clara, CA, USA). Signal intensity from the somatic area of each cell was background subtracted by removing the average signal from an area adjacent the cell imaged but devoid of cellular components. Ratios were then converted to absolute Ca^{2+} levels using the following equation $[Ca^{2+}] = K_D\beta\ (R-R_{min})/(R_{max}-R)$ where R is the 340/380 emission ratio, and R_{min} and R_{max} represent ratios of the lowest and the highest standard Ca^{2+} concentration imaged (respectively). Calibration of the ratios was accomplished using a series of increasing free Ca^{2+} concentrations from 0 to 39 μM containing 1 mM Mg^{2+}(Invitrogen). R_{min}, R_{max}, and $K_D\beta$ were determined by fitting ratios from the calibration curve with a 4-terms sigmoid function (SigmaPlot, Systat, Chicago, IL, USA), and were 0.29, 5.17, and 2.14 μM, respectively.

Drugs and drug delivery

Thiazolidinedione concentrations and exposure durations were chosen to match conditions where these drugs are protective in culture (Uryu *et al.* 2002; Dello Russo *et al.* 2003; Camacho *et al.* 2004), take into consideration the higher affinity of rosiglitazone (ROSI) for PPAR-γ compared to pioglitazone (PIO) (Willson *et al.* 1996; Awais *et al.* 2007), and are clinically relevant (Asano *et al.* 1999; Brunton *et al.* 2005; Feinstein *et al.* 2005). ROSI and T0070907 (TIO) were purchased from Cayman Chemical (Ann Arbor, MI, USA). TIO, a selective/irreversible PPAR-γ antagonist promotes the recruitment of co-repressors and blocks agonist-induced recruitment of co-activators (Lee *et al.* 2002). PIO was donated by MW Kilgore. These drugs were dissolved in DMSO and stored at −20°C until used as a 1 : 1000 dilution into cell culture medium. Cells were washed twice following exposure (2, 24, 72 h) and TZDs were absent during Ca^{2+} imaging or electrophysiological experiments. Vehicle-treated cultures were exposed to 0.1% DMSO for similar times. NMDA (Sigma-Aldrich, St. Louis, MO, USA) was

dissolved in water and stored at −20°C. All other drugs and salts were purchased from Sigma-Aldrich and were dissolved in HPLC-grade water. NMDAR-mediated Ca^{2+} currents and transients were recorded in response to NMDA exposure delivered with a SF77A rapid solution exchange system (Warner Instruments Corp., Hamden, CT, USA). This system is composed of a computer-controlled stepper motor which rapidly switches the position of separate glass barrels (700 micron-wide) carrying a constant stream of recording solutions across the cells (~300 μL/min). Barrels are placed ~ 75 microns above the cells and control the environment surrounding the cells. For NMDAR-mediated currents, a 500 ms, 300 μM NMDA exposure was used, and for Ca^{2+} imaging, a 5 s application of the same concentration was used. This NMDA concentration was chosen because it induces maximal currents in hippocampal cultures recorded at this DIV (Brewer *et al.* 2007).

Statistics

Cells with membrane resistance < 300 MΩ, holding current > 200 pA (from −70 mV holding potential) or resting Ca^{2+} levels > 200 nM were removed from the analysis. Effects of treatments on electrophysiologic and imaging variables were assessed with one-way ANOVA (with repeated measure as noted) using Prism (GraphPad software, La Jolla, CA, USA). Tukey's *post-hoc* test was used for pairwise comparisons. A one-way ANOVA by rank analysis (Kruskal-Wallis) was used for statistical comparisons on DNA binding fold change analyses, and a *t*-test was used for analysis of western blots. All data presented in graph form represent means ± SEM.

Results

PPAR-γ DNA binding and PPAR-γ protein expression

In order to assess the involvement of PPAR-γ activation in response to TZD treatment, we monitored DNA binding using nuclear extracts from hippocampal neurons treated 24 h with vehicle (0.1% DMSO), PIO (0.1–10 μM), or ROSI (1 μM). Nuclear extracts were hybridized to an ELISA-based PPAR-γ assay which quantifies PPAR-γ DNA binding to PPREs (Fig. 1a). The significant increase in DNA binding following 24 h treatment with 10 μM PIO (ANOVA, $p < 0.05$) was reduced by the selective PPAR-γ antagonist TIO (1 μM). Treatment of cultures with TIO alone did not reduce PPAR-γ DNA binding below control conditions (ANOVA, $p > 0.05$), indicating little endogenous PPAR-γ activation is present in hippocampal cultures. Surprisingly, at 24 h treatment with 1 μM ROSI, DNA binding was not enhanced while nuclear PPAR-γ protein levels were elevated, as reported by western blot techniques (Fig. 1b). Because ROSI did not enhance DNA binding, we did not test for reversibility with a combination of ROSI and TIO. These results suggest that selective modulation of PPAR-γ via different agonists may affect DNA binding and protein expression differently (see Discussion). Furthermore, results from the TIO experiments indicate that under the conditions tested, the antagonist can significantly reduce DNA binding. In subsequent experiments, we use this antagonist to test the dependence of PIO and ROSI's effects on VGCCs and NMDARs through PPAR-γ activation.

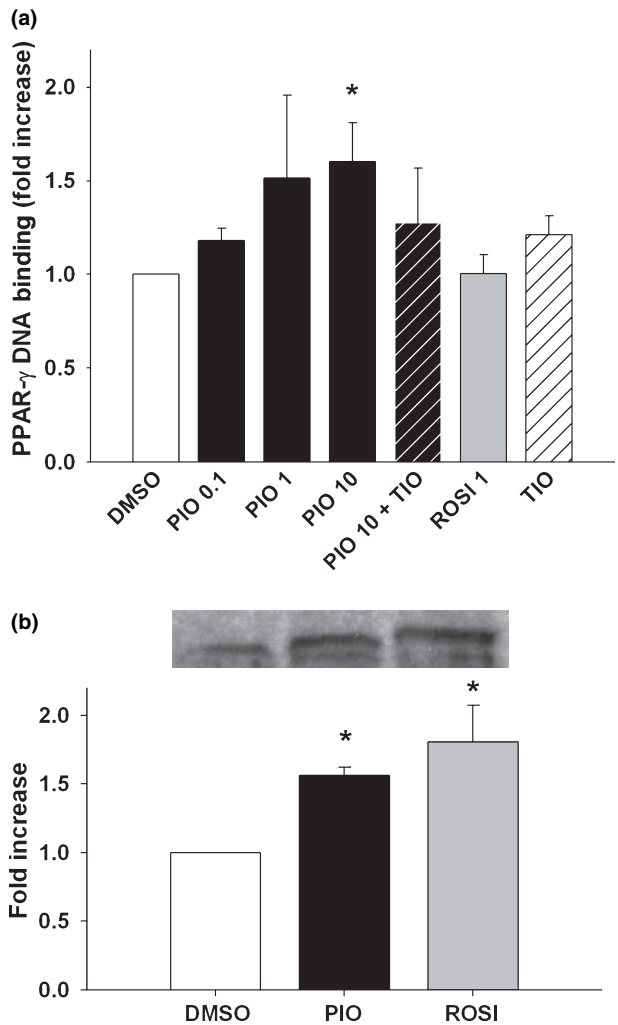

Fig. 1 Effects of PIO and ROSI on PPAR-γ DNA binding and protein expression. (a) shows dose-dependent increase in PPAR-γ DNA binding in response to 24 h treatment with increasing concentrations of pioglitazone (PIO) or rosiglitazone (ROSI). T0070907 (TIO) the selective PPAR-γ antagonist prevented binding. Statistical comparisons were made against a vehicle treatment group (0.1% DMSO) (n = 3–15/group, $^*p < 0.05$, ANOVA). (b) shows a representative western blot (top) and group data responses (bottom) to 24 h treatment with 10 μM PIO or 1 μM ROSI (n = 3/group, $^*p < 0.05$, *t*-test).

Rosiglitazone but not pioglitazone reduces VGCC currents

We used patch clamping techniques on hippocampal neurons treated 24 h with PIO or ROSI to record VGCC currents and monitor the effects of these two TZDs. Figure 2 shows representative examples of VGCC current traces (a, c, e), mean VGCC current densities (b, d, f), and *I/V* relationships (g) measured across several treatment conditions. No main effect of drug on VGCC current

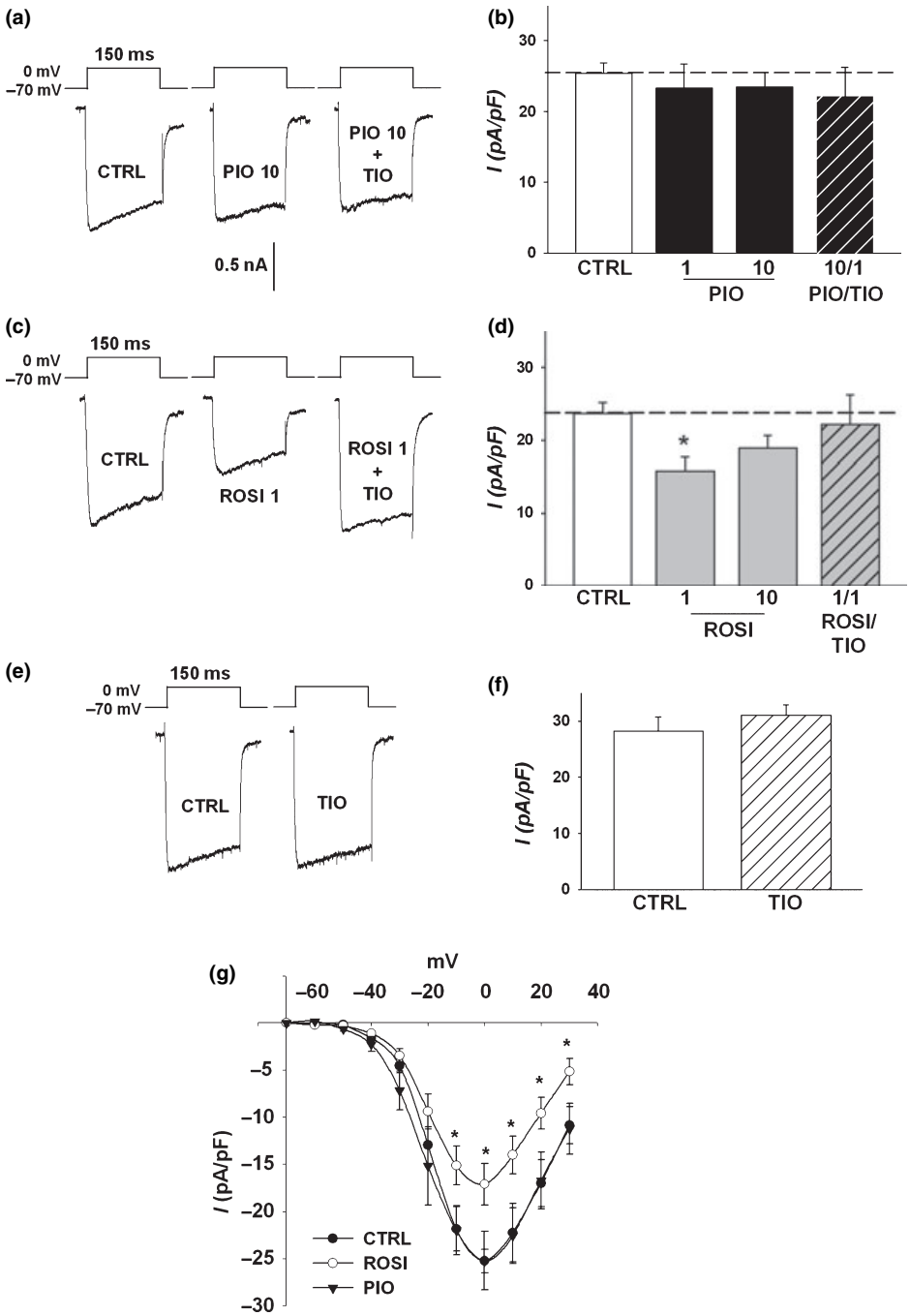

Fig. 2 Effects of 24 h treatment with TZDs on VGCC currents. (a), (c) and (e) show representative examples of whole-cell currents elicited upon depolarization from −70 to 0 mV for 150 ms (voltage steps are shown above each trace). (b), (d) and (f) show peak current densities (mean ± SEM) recorded across several treatment conditions. Dashed line represents the peak current density measured in control cells. ROSI 1 μM, but not PIO significantly reduced peak current densities. While TIO did not change peak current density when tested alone, it was able to prevent the inhibition caused by ROSI (d). Asterisks indicates significant difference from the vehicle-treated group (0.1% DMSO-CTRL), (n = 10–47 neurons/group; $p < 0.01$; ANOVA). *I/V* relationship analysis shows ROSI, while inhibiting peak current densities (*$p \leq 0.05$; Tukey's *post-hoc* test), did not shift VGCC current activation.

density (Fig. 2b) or passive membrane properties (Table 1) were detected at three concentrations of PIO tested (0.1 not shown, 1 and 10 μM; ANOVA, $p > 0.05$). Similar results were seen with 2 h (n = 7–12), or 72 h (n = 15–17) PIO treatment at 10 μM (data not shown). In contrast, 24 h ROSI treatment significantly reduced VGCC current density

Table 1 Passive membrane properties

Group	Cm (pF)	Rm (MΩ)	Ra (MΩ)	HC (pA)
CTRL	75.0 ± 3.2	543.5 ± 24.0	6.7 ± 0.3	−73.0 ± 6.6
PIO 1 μM	61.4 ± 3.9	504.0 ± 54.1	7.0 ± 0.7	−109.0 ± 20.1
PIO 10 μM	82.0 ± 5.6	519.0 ± 33.0	7.1 ± 0.4	−92.4 ± 18.6
PIO 10 μM + TIO 1 μM	67.7 ± 5.4	628.6 ± 58.0	4.4 ± 0.7	−50.6 ± 11.5
ROSI 1 μM	78.6 ± 3.3	453.3 ± 33.7	7.3 ± 0.6	−89.0 ± 14.7
ROSI 1 μM + TIO 1 μM	74.0 ± 5.8	546.1 ± 80.0	5.8 ± 0.6	−84.7 ± 21.0
ROSI 10 μM	62.6 ± 6.4	464.4 ± 22.0	5.8 ± 0.7	−81.5 ± 12.2
TIO 1 μM	64.1 ± 4.4	661.0 ± 64.9	6.8 ± 0.5	−52.0 ± 8.8

Values represent means ± SEM on measures of membrane capacitance (Cm), membrane resistance (Rm), access resistance (Ra), and holding current (HC) necessary to hold a cell at −70 mV (n = 10–52 cells/group). No significant difference was found in any of these parameters across treatment groups ($p > 0.05$, one-way ANOVA).

measured from −70 mV (Fig. 2d; ANOVA; $p < 0.05$) or −40 mV (data not shown). Interestingly, greater ROSI-mediated VGCC inhibition was noted on currents elicited from −40 mV compared to −70 mV (data not shown, $p < 0.0005$), suggesting high voltage-activated L-type currents might be more sensitive than low voltage-activated Ca^{2+} currents to the inhibitory effects of ROSI. In vascular myocytes, rapid PPAR-γ-independent inhibitory effects of ROSI on L-VGCC currents have been observed (Knock *et al.* 1999). A direct effect of ROSI on L-VGCC is not likely the mechanism of inhibition reported here, however, because co-treatment of cultures with ROSI (1 μM) and the PPAR-γ antagonist TIO (1 μM) for 24 h, was able to completely reverse ROSI's effects on VGCCs (Fig. 2d). Further, ROSI was not present during these experiments. TIO alone for 24 h (n = 18), or ROSI for 2 h (n = 6, data not shown) had no detectable effect on VGCC current densities (Fig. 2e and f). As seen in the *I/V* relationship analysis (Fig. 2g), ROSI inhibited peak currents density but did not shift the activation curve and voltage-sensitivity of the currents. Taken together, these data demonstrate that ROSI's effects on VGCC are dependent on PPAR-γ activation, and also suggest little basal PPAR-γ modulation of these Ca^{2+} currents.

Pioglitazone but not rosiglitazone reduces NMDAR-induced Ca^{2+} currents

We assessed the effect of PIO and ROSI on NMDAR-mediated Ca^{2+} currents, another primary source of Ca^{2+} in hippocampal neurons. Figure 3 shows representative NMDA-induced Ca^{2+} current traces (a, c, e) and mean current densities (b, d, f) measured across several treatment conditions. Compared to control-treated cells, 24 h PIO treatment significantly reduced NMDAR-induced Ca^{2+} currents (500 ms, 300 μM NMDA exposure) (Fig. 3a and b; ANOVA; $p < 0.05$). This effect was prevented with co-treatment of cultures using both PIO (10 μM) and TIO (1 μM) for 24 h. TIO alone for 24 h (n = 11) did not modify NMDA-induced Ca^{2+} currents (Fig. 3e and f), suggesting that there is little PPAR-γ tone on hippocampal neurons in these culture conditions. Conversely, 24 h ROSI treatment did not reduce NMDAR-induced currents (Fig. 3d; ANOVA; $p > 0.05$). For this reason, we did not monitor Ca^{2+} levels during NMDA application following a 24 h ROSI treatment. These data show that NMDARs are a novel target of PIO whose inhibition appears dependent on PPAR-γ activation.

Pioglitazone reduces NMDAR-mediated Ca^{2+} levels

In order to identify whether the effects reported thus far could have an impact on Ca^{2+} homeostasis during NMDAR-mediated activation, we monitored intracellular Ca^{2+} levels using the ratiometric Ca^{2+} indicator Fura-2. Effects of chronic PIO (24 h) treatment on NMDAR-induced intracellular Ca^{2+} elevations (5 s, 300 μM NMDA exposure) were measured and compared to control conditions. In response to NMDA, robust increases in $[Ca^{2+}]$ (∼ 2.0 μM) were seen in cells treated 24 h with 0.1% DMSO, however, the same NMDA exposure yielded much reduced (∼1.4 μM) $[Ca^{2+}]$ in cells treated 24 h with 10 μM PIO (Fig. 4). While a significant reduction in $[Ca^{2+}]$ was seen during the NMDA exposure (ANOVA; $p < 0.0001$), PIO had no effect on resting Ca^{2+} concentrations. These results are consistent with the interpretation that PIO's neuroprotective effects might be mediated, at least in part, by rectification of Ca^{2+} homeostasis during an insult.

Discussion

Elevated and long-lasting increases in cytoplasmic $[Ca^{2+}]$ are consistent biomarkers of aging that represent one aspect of neuronal Ca^{2+} dyshomeostasis (Kirischuk and Verkhratsky 1996; Thibault *et al.* 2001; Murchison *et al.* 2004; Hemond and Jaffe 2005; Gant *et al.* 2006). Enhanced Ca^{2+} transients are also present in AD models (Mattson and Guo 1997; LaFerla 2002; Stutzmann *et al.* 2007; Cheung *et al.* 2008) and in cells from AD patients (Ito *et al.* 1994; Gibson *et al.* 1996; Hirashima *et al.* 1996; Etcheberrigaray *et al.* 1998). Because VGCC and NMDAR blockers show improved cognition in animal models of aging (Deyo *et al.* 1989;

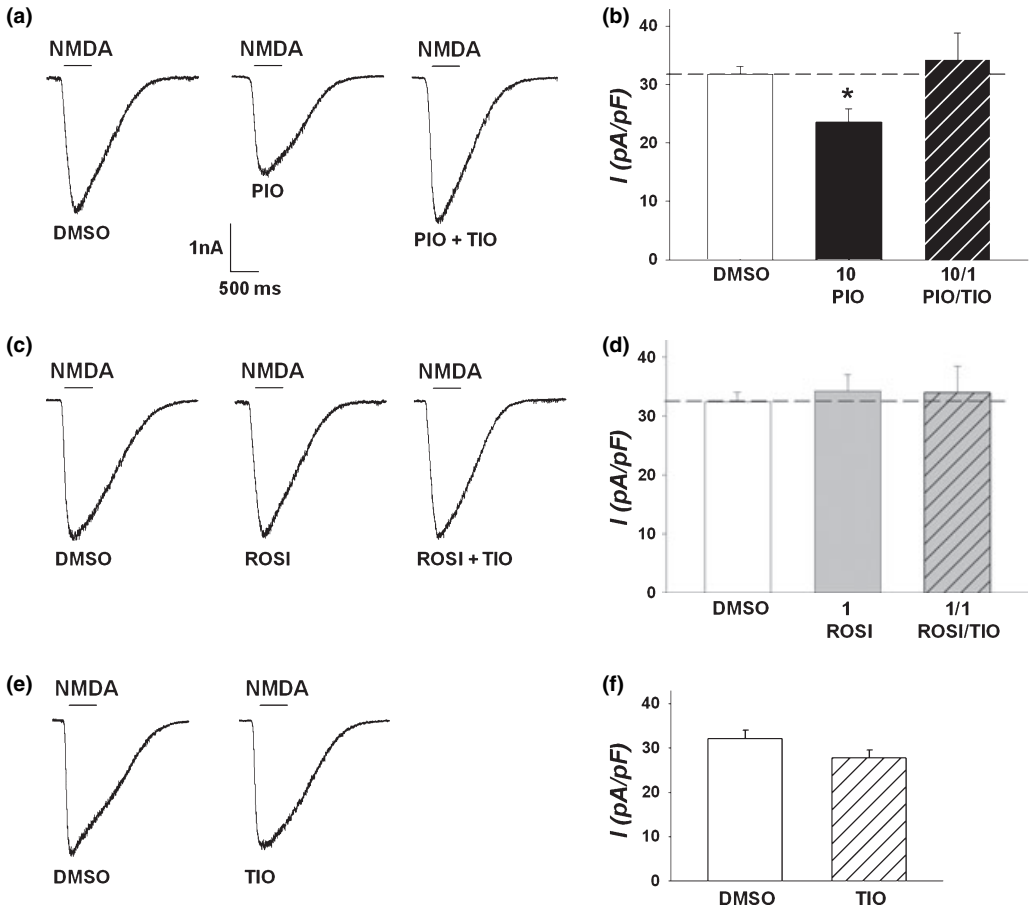

Fig. 3 Twenty-four hour PIO reduces NMDAR-mediated currents. (a), (c) and (e) show representative current traces in response to a 500 ms, 300 μM NMDA pulse (horizontal bar). Cultures were treated either with DMSO (0.1%), PIO (10 μM), ROSI (1 μM), or TIO (1 μM) alone or in combination with the agonists. (b), (d) and (f) show corresponding mean group current density data (means ± SEM) recorded under these treatment conditions (n = 6–34). While PIO significantly reduced NMDAR-mediated current density (*$p < 0.05$; ANOVA), ROSI had no significant effect (c and d). The PIO effect on NMDAR-mediated current was prevented when TIO was added in combination with PIO for 24 h. TIO alone did not affect NMDA-induced Ca^{2+} currents (f).

Moyer *et al.* 1992; Kowalska and Disterhoft 1994), and can reduce risk of dementia in hypertensive or AD patients (Forette *et al.* 2002; Reisberg *et al.* 2003; Lipton 2004), we sought to test the hypothesis that TZDs could reduce Ca^{2+} signaling in neurons. Furthermore, while there has been some reports that PPAR-γ agonists (including ROSI) reduce [Ca^{2+}] during Aβ-mediated insults in cortical neurons (Inestrosa *et al.* 2005), neither troglitazone nor the endogenous PPAR-γ agonist 15d-PGJ2 appear to reduce [Ca^{2+}] during an NMDA-mediated insult (Uryu *et al.* 2002; Zhao *et al.* 2006). We show here that indeed, TZDs can have very different effects, and that the only two clinically-relevant TZDs approved for the treatment of T2DM (ROSI and PIO) reduce Ca^{2+} flux into hippocampal neurons by targeting two different ion channels. PIO reduced NMDAR-mediated Ca^{2+} currents and transients but had little to no impact on VGCC currents. Conversely, ROSI reduced VGCC currents, but not NMDAR-mediated currents.

Pioglitazone's effects on NMDAR-mediated currents and Ca^{2+} transients provide evidence for new mechanisms associated with its neuroprotective effects. It is well documented that Ca^{2+}-mediated toxicity (excitotoxicity) occurs in response to prolonged activation of NMDARs (Choi *et al.* 1988; Mattson *et al.* 1991; Lipton and Rosenberg 1994; Olney 2002) and that NMDAR antagonism, provides neuroprotection in several culture models of aging and neurodegeneration, by reducing Ca^{2+} levels during an insult (Choi *et al.* 1988; Levy and Lipton 1990; Zhou and Baudry 2006; Brewer *et al.* 2007). Use of the low affinity uncompetitive NMDAR antagonist memantine has been associated with a slowing of disease progression in patients with moderate-to-severe forms of AD (Reisberg *et al.* 2003). Thus, one of PIO's neuroprotective actions might be mediated, in part, by a reduction in NMDAR-mediated Ca^{2+} currents and levels, particularly in conditions associated with NMDA over-activation (e.g., neurodegeneration, ischemia, and stroke). Further, because

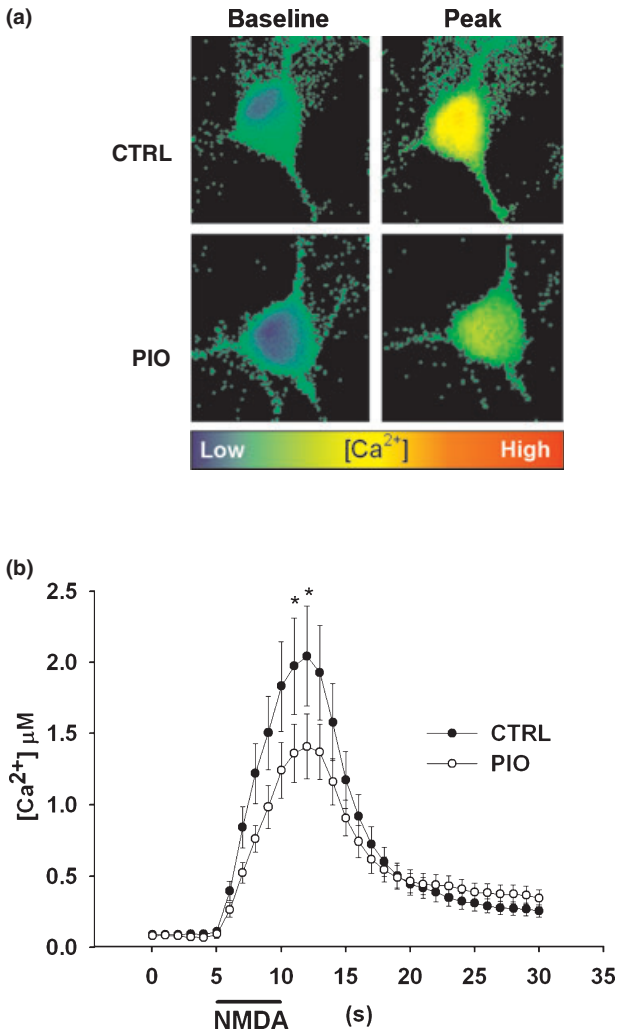

Fig. 4 Twenty-four hour PIO treatment reduces intracellular NMDA-induced [Ca^{2+}]. (a) shows representative Fura-2-loaded hippocampal neurons used for ratiometric analyses on intracellular Ca^{2+} concentrations taken before (baseline), and during (peak) NMDA exposure (300 μM, 5 s) in control-treated (CTRL) and PIO-treated cells. (b) shows group data in control-treated (CTRL) and PIO-treated cells (n = 32–35) imaged before, during (thick horizontal bar) and after NMDA exposure (*$p < 0.05$; Tukey's *post-hoc* test).

PIO's effect on Ca^{2+} currents was reversed by the PPAR-γ antagonist TIO (Fig. 3a and b), the underlying mechanism appears to be transcriptionally mediated.

In contrast to PIO, ROSI specifically reduced Ca^{2+} signaling through VGCCs. As shown in Fig. 2, this effect was precluded by TIO treatment, indicating that ROSI's effects on VGCCs also are transcriptionally regulated. These results provide insights into the mechanisms underlying ROSI's effects on cognition. Functional memory improvement has been seen in response to ROSI treatment *in vivo* (see introduction), and it is tempting to speculate that this effect might be mediated by reduction of signaling through VGCC. Indeed, use of VGCC blockers (e.g., dihydropyridines) is associated with improved learning and memory in animal models of aging (Deyo *et al.* 1989; Moyer *et al.* 1992; Kowalska and Disterhoft 1994). In humans, use of VGCC blockers for the treatment of hypertension has been associated with a significant improvement in cognition (Trompet *et al.* 2008), and a reduced risk for developing dementia (Forette *et al.* 2002; Khachaturian *et al.* 2006). However, because ROSI does not appear to appreciably cross the blood brain barrier (Maeshiba *et al.* 1997; Pedersen *et al.* 2006), prior beneficial effects of ROSI on brain function have mostly been attributed to peripheral actions, such as reestablishment of normal glucose (Pedersen and Flynn 2004; Ryan *et al.* 2006) or insulin levels (Watson *et al.* 2005; Risner *et al.* 2006). Still, peripherally administered ROSI has been shown to increase PPAR-γ DNA binding in the brain (Luo *et al.* 2006), and may more readily gain access under conditions associated with a weakened blood brain barrier such as aging/AD (Gemma *et al.* 2004; Watson *et al.* 2005). Irrespective of its pharmacokinetic profile, ROSI's reduction in VGCC function in the brain may represent a new and beneficial mechanism of action which draws a parallel with the use of L-type VGCC blockers and their association with a decreased incidence of dementia.

Thiazolidinediones have been shown to activate both PPAR-γ-dependent and independent pathways in the brain (Feinstein *et al.* 2005; Sundararajan *et al.* 2006; Kapadia *et al.* 2008). We show here that treatment of hippocampal cultures with PIO increases PPAR-γ binding to PPREs at 24 h, and that this event is significantly reduced by TIO (Fig. 1). Further, the effects reported here on VGCC- and NMDAR-mediated Ca^{2+} homeostasis occurred in the absence of PIO or ROSI in the recording medium and are sensitive to TIO (Figs 2 and 3). Also, 2 h treatment with either drugs did not affect VGCC recordings. Together, these results are consistent with effects of TZDs occurring through classic nuclear receptor binding. Indeed, numerous reports have identified receptor-dependent beneficial aspects of TZD use, including reduced neuronal Ca^{2+} levels during Aβ-mediated insults through activation of Wnt signaling (Inestrosa *et al.* 2005), reduced inflammation in models of neurodegeneration through suppression of proinflammatory genes and proteins (Combs *et al.* 2000; Daynes and Jones 2002; Heneka *et al.* 2005), and suppression of inducible nitric oxide synthase (Heneka *et al.* 2000). Our results emphasize a TZD-mediated reduction in Ca^{2+} overload which could act complementarily with mechanisms of anti-inflammation or anti-oxidation. In fact, a synergistic pathway between the NMDAR antagonist MK-801 and ROSI has been identified, where drug combination therapy improves neurological outcome when compared to either compound administered alone (Allahtavakoli *et al.* 2007). Nevertheless, in the brain there has been several reports of non-PPAR-γ-dependent effects of TZDs, including rapid effects on mitochondrial function (Dello Russo *et al.* 2003; Colca

et al. 2004; Feinstein *et al.* 2005; Hunter *et al.* 2008) and oxidative stress (Aoun *et al.* 2003), and further studies are necessary to identify whether these pathways can co-exist.

Our results demonstrate the presence of a 'double dissociation' between the effects of PIO and ROSI on VGCCs and NMDARs, albeit through a single receptor. Interestingly, while PIO and ROSI increased PPAR-γ protein levels at 24 h, results from PPRE binding assay did not follow that profile (Fig. 1). Structural differences between PIO and ROSI are likely to mediate the double dissociation seen here, given that separate ligands for the same nuclear receptor can differently alter the conformation of that receptor and mediate unique biological responses (Nolte *et al.* 1998; Gani and Sylte 2008). In fact, the development of selective estrogen receptor modulators is the basis for major drug discovery efforts in the treatment of breast cancer and osteoporosis (Riggs and Hartmann 2003). Similarly, selective PPAR-γ modulators (Rangwala and Lazar 2002; Zhang *et al.* 2007) also have been reported to alter the recruitment of co-activators/repressors in different tissues and mediate distinct gene expression profiles (Nolte *et al.* 1998; Norris *et al.* 1999; Paige *et al.* 1999). Under these conditions, selective PPAR-γ modulators appear able to impart distinct physiological responses in breast cancer cells (Thoennes *et al.* 2000; Allred and Kilgore 2005). Thus we believe the effects of ROSI and PIO on two different ion channels, while dependent on PPAR-γ, as evidenced by their sensitivity to TIO, are likely mediated by subtle structural changes in the agonists, changes in co-activators/repressors recruitment, and/or changes in the duration of the signal (Feige *et al.* 2005; Gani and Sylte 2008).

The present study demonstrates novel and potentially beneficial actions of two TZDs used clinically for the treatment of T2DM. While their conventional mechanism of action is associated with reestablishing insulin sensitivity in peripheral tissues, we show here that NMDAR and VGCC pathways are novel brain targets of TZDs whose inhibition may account, at least in part, for the therapeutic neurological benefits associated with use of these compounds. Both NMDARs and VGCCs are key participants in learning and memory processes and have also been shown to be altered with aging and/or AD. Therefore, TZDs may have potential applications in conditions associated with impaired learning and memory.

Acknowledgements

We thank Drs. Hadley and Brewer for their critical reading and valuable input on the manuscript. We thank Dr. Wang for her technical expertise on the DNA binding assay, and Dr. S. Kraner for the modifications she recommended on the assay protocol. This study was supported by grants AG029268, NCRR-P20-RR15592, and a gift from the Neurosciences Education and Research Foundation.

References

Allahtavakoli M., Shabanzadeh A., Roohbakhsh A. and Pourshanazari A. (2007) Combination therapy of rosiglitazone, a peroxisome proliferator-activated receptor-gamma ligand, and NMDA receptor antagonist (MK-801) on experimental embolic stroke in rats. *Basic Clin. Pharmacol. Toxicol.* **101**, 309–314.

Allred C. D. and Kilgore M. W. (2005) Selective activation of PPAR-gamma in breast, colon, and lung cancer cell lines. *Mol. Cell. Endocrinol.* **235**, 21–29.

Aoun P., Watson D. G. and Simpkins J. W. (2003) Neuroprotective effects of PPARgamma agonists against oxidative insults in HT-22 cells. *Eur. J. Pharmacol.* **472**, 65–71.

Asano M., Nakajima T., Iwasawa K. *et al.* (1999) Troglitazone and pioglitazone attenuate agonist-dependent Ca2+ mobilization and cell proliferation in vascular smooth muscle cells. *Br. J. Pharmacol.* **128**, 673–683.

Awais M., Sato M. and Umezawa Y. (2007) A fluorescent indicator to visualize ligand-induced receptor/coactivator interactions for screening of peroxisome proliferator-activated receptor gamma ligands in living cells. *Biosens. Bioelectron.* **22**, 2564–2569.

Berger J. and Moller D. E. (2002) The mechanisms of action of PPARs. *Annu. Rev. Med.* **53**, 409–435.

Berger J. P., Akiyama T. E. and Meinke P. T. (2005) PPARs: therapeutic targets for metabolic disease. *Trends Pharmacol. Sci.* **26**, 244–251.

Biessels G. J., Kamal A., Urban I. J., Spruijt B. M., Erkelens D. W. and Gispen W. H. (1998) Water maze learning and hippocampal synaptic plasticity in streptozotocin-diabetic rats: effects of insulin treatment. *Brain Res.* **800**, 125–135.

Biessels G. J., Staekenborg S., Brunner E., Brayne C. and Scheltens P. (2006) Risk of dementia in diabetes mellitus: a systematic review. *Lancet Neurol.* **5**, 64–74.

Brewer L. D., Thibault O., Staton J., Thibault V., Rogers J. T., Garcia-Ramos G., Kraner S., Landfield P. W. and Porter N. M. (2007) Increased vulnerability of hippocampal neurons with age in culture: temporal association with increases in NMDA receptor current, NR2A subunit expression and recruitment of L-type calcium channels. *Brain Res.* **1151**, 20–31.

Brunton L. L., Sazo J. S. and Parker K. L. (2005) *Goodman and Gilman's The Pharmacological Basis of Therapeutics*, 11th edn, pp. 1860. McGraw-Hill Professional, New York, NY.

Camacho I. E., Serneels L., Spittaels K., Merchiers P., Dominguez D. and De Strooper B. (2004) Peroxisome-proliferator-activated receptor gamma induces a clearance mechanism for the amyloid-beta peptide. *J. Neurosci.* **24**, 10908–10917.

Cheung K. H., Shineman D., Muller M. *et al.* (2008) Mechanism of Ca2+ disruption in Alzheimer's disease by presenilin regulation of InsP(3) receptor channel gating. *Neuron* **58**, 871–883.

Choi D. W., Koh J. Y. and Peters S. (1988) Pharmacology of glutamate neurotoxicity in cortical cell culture: attenuation by NMDA antagonists. *J. Neurosci.* **8**, 185–196.

Cimini A., Benedetti E., Cristiano L., Sebastiani P., D'Amico M. A., D'Angelo B. and Di Loreto S. (2005) Expression of peroxisome proliferator-activated receptors (PPARs) and retinoic acid receptors (RXRs) in rat cortical neurons. *Neuroscience* **130**, 325–337.

Colca J. R., McDonald W. G., Waldon D. J., Leone J. W., Lull J. M., Bannow C. A., Lund E. T. and Mathews W. R. (2004) Identification of a novel mitochondrial protein ("mitoNEET") cross-linked specifically by a thiazolidinedione photoprobe. *Am. J. Physiol. Endocrinol. Metab.* **286**, E252–E260.

Combs C. K., Johnson D. E., Karlo J. C., Cannady S. B. and Landreth G. E. (2000) Inflammatory mechanisms in Alzheimer's disease: inhibition of beta-amyloid-stimulated proinflammatory responses

and neurotoxicity by PPARgamma agonists. *J. Neurosci.* **20**, 558–567.

Daynes R. A. and Jones D. C. (2002) Emerging roles of PPARs in inflammation and immunity. *Nat. Rev. Immunol.* **2**, 748–759.

Dello Russo C., Gavrilyuk V., Weinberg G., Almeida A., Bolanos J. P., Palmer J., Pelligrino D., Galea E. and Feinstein D. L. (2003) Peroxisome proliferator-activated receptor gamma thiazolidinedione agonists increase glucose metabolism in astrocytes. *J. Biol. Chem.* **278**, 5828–5836.

Deyo R. A., Straube K. T. and Disterhoft J. F. (1989) Nimodipine facilitates associative learning in aging rabbits. *Science* **243**, 809–811.

Disterhoft J. F., Thompson L. T., Moyer J. R. Jr and Mogul D. J. (1996) Calcium-dependent afterhyperpolarization and learning in young and aging hippocampus. *Life Sci.* **59**, 413–420.

Etcheberrigaray R., Hirashima N., Nee L., Prince J., Govoni S., Racchi M., Tanzi R. E. and Alkon D. L. (1998) Calcium responses in fibroblasts from asymptomatic members of Alzheimer's disease families. *Neurobiol. Dis.* **5**, 37–45.

Feige J. N., Gelman L., Tudor C., Engelborghs Y., Wahli W. and Desvergne B. (2005) Fluorescence imaging reveals the nuclear behavior of peroxisome proliferator-activated receptor/retinoid X receptor heterodimers in the absence and presence of ligand. *J. Biol. Chem.* **280**, 17880–17890.

Feinstein D. L. (2003) Therapeutic potential of peroxisome proliferator-activated receptor agonists for neurological disease. *Diabetes Technol. Ther.* **5**, 67–73.

Feinstein D. L., Spagnolo A., Akar C., Weinberg G., Murphy P., Gavrilyuk V. and Dello Russo C. (2005) Receptor-independent actions of PPAR thiazolidinedione agonists: is mitochondrial function the key? *Biochem. Pharmacol.* **70**, 177–188.

Forette F., Seux M. L., Staessen J. A. *et al.* (2002) The prevention of dementia with antihypertensive treatment: new evidence from the Systolic Hypertension in Europe (Syst-Eur) study. *Arch. Intern. Med.* **162**, 2046–2052.

Fuenzalida K., Quintanilla R., Ramos P., Piderit D., Fuentealba R. A., Martinez G., Inestrosa N. C. and Bronfman M. (2007) Peroxisome proliferator-activated receptor gamma up-regulates the Bcl-2 anti-apoptotic protein in neurons and induces mitochondrial stabilization and protection against oxidative stress and apoptosis. *J. Biol. Chem.* **282**, 37006–37015.

Gani O. A. and Sylte I. (2008) Ligand-induced stabilization and activation of peroxisome proliferator-activated receptor gamma. *Chem. Biol. Drug. Des.* **72**, 50–57.

Gant J. C., Sama M. M., Landfield P. W. and Thibault O. (2006) Early and simultaneous emergence of multiple hippocampal biomarkers of aging is mediated by Ca2+-induced Ca2+ release. *J. Neurosci.* **26**, 3482–3490.

Garcia-Bueno B., Madrigal J. L., Lizasoain I., Moro M. A., Lorenzo P. and Leza J. C. (2005) Peroxisome proliferator-activated receptor gamma activation decreases neuroinflammation in brain after stress in rats. *Biol. Psychiatry* **57**, 885–894.

Gardoni F., Kamal A., Bellone C., Biessels G. J., Ramakers G. M., Cattabeni F., Gispent W. H. and Di Luca M. (2002) Effects of streptozotocin-diabetes on the hippocampal NMDA receptor complex in rats. *J. Neurochem.* **80**, 438–447.

Gasparini L., Netzer W. J., Greengard P. and Xu H. (2002) Does insulin dysfunction play a role in Alzheimer's disease? *Trends Pharmacol. Sci.* **23**, 288–293.

Gemma C., Stellwagen H., Fister M., Coultrap S. J., Mesches M. H., Browning M. D. and Bickford P. C. (2004) Rosiglitazone improves contextual fear conditioning in aged rats. *Neuroreport* **15**, 2255–2259.

Gibson G. E., Zhang H., Toral-Barza L., Szolosi S. and Tofel-Grehl B. (1996) Calcium stores in cultured fibroblasts and their changes with Alzheimer's disease. *Biochim. Biophys. Acta* **1316**, 71–77.

Hauner H. (2002) The mode of action of thiazolidinediones. *Diabetes Metab. Res. Rev.* **18**(Suppl 2), S10–S15.

Hemond P. and Jaffe D. B. (2005) Caloric restriction prevents aging-associated changes in spike-mediated Ca2+ accumulation and the slow afterhyperpolarization in hippocampal CA1 pyramidal neurons. *Neuroscience* **135**, 413–420.

Heneka M. T., Klockgether T. and Feinstein D. L. (2000) Peroxisome proliferator-activated receptor-gamma ligands reduce neuronal inducible nitric oxide synthase expression and cell death in vivo. *J. Neurosci.* **20**, 6862–6867.

Heneka M. T., Sastre M., Dumitrescu-Ozimek L. *et al.* (2005) Acute treatment with the PPAR{gamma} agonist pioglitazone and ibuprofen reduces glial inflammation and A{beta}1-42 levels in APPV717I transgenic mice. *Brain* **128**, 1442–1453.

Hirashima N., Etcheberrigaray R., Bergamaschi S., Racchi M., Battaini F., Binetti G., Govoni S. and Alkon D. L. (1996) Calcium responses in human fibroblasts: a diagnostic molecular profile for Alzheimer's disease. *Neurobiol. Aging* **17**, 549–555.

Hofmann C., Lorenz K., Braithwaite S. S., Colca J. R., Palazuk B. J., Hotamisligil G. S. and Spiegelman B. M. (1994) Altered gene expression for tumor necrosis factor-alpha and its receptors during drug and dietary modulation of insulin resistance. *Endocrinology* **134**, 264–270.

Hoyer S. (2004) Glucose metabolism and insulin receptor signal transduction in Alzheimer disease. *Eur. J. Pharmacol.* **490**, 115–125.

Huang T. J., Sayers N. M., Fernyhough P. and Verkhratsky A. (2002) Diabetes-induced alterations in calcium homeostasis in sensory neurones of streptozotocin-diabetic rats are restricted to lumbar ganglia and are prevented by neurotrophin-3. *Diabetologia* **45**, 560–570.

Huang T. J., Sayers N. M., Verkhratsky A. and Fernyhough P. (2005) Neurotrophin-3 prevents mitochondrial dysfunction in sensory neurons of streptozotocin-diabetic rats. *Exp. Neurol.* **194**, 279–283.

Hunter R. L., Dragicevic N., Seifert K., Choi D. Y., Liu M., Kim H. C., Cass W. A., Sullivan P. G. and Bing G. (2007) Inflammation induces mitochondrial dysfunction and dopaminergic neurodegeneration in the nigrostriatal system. *J. Neurochem.* **100**, 1375–1386.

Hunter R. L., Choi D. Y., Ross S. A. and Bing G. (2008) Protective properties afforded by pioglitazone against intrastriatal LPS in Sprague-Dawley rats. *Neurosci. Lett.* **432**, 198–201.

Inestrosa N. C., Godoy J. A., Quintanilla R. A., Koenig C. S. and Bronfman M. (2005) Peroxisome proliferator-activated receptor gamma is expressed in hippocampal neurons and its activation prevents beta-amyloid neurodegeneration: role of Wnt signaling. *Exp. Cell Res.* **304**, 91–104.

Ito E., Oka K., Etcheberrigaray R., Nelson T. J., McPhie D. L., Tofel-Grehl B., Gibson G. E. and Alkon D. L. (1994) Internal Ca^{2+} mobilization is altered in fibroblasts from patients with Alzheimer disease. *Proc. Natl Acad. Sci. USA*, **91**, 534–538.

Janson J., Laedtke T., Parisi J. E., O'Brien P., Petersen R. C. and Butler P. C. (2004) Increased risk of type 2 diabetes in Alzheimer disease. *Diabetes* **53**, 474–481.

Jiang Q., Heneka M. and Landreth G. E. (2008) The role of peroxisome proliferator-activated receptor-gamma (PPARgamma) in Alzheimer's disease: therapeutic implications. *CNS Drugs* **22**, 1–14.

Kamal A., Artola A., Biessels G. J., Gispen W. H. and Ramakers G. M. (2003) Increased spike broadening and slow afterhyperpolarization in CA1 pyramidal cells of streptozotocin-induced diabetic rats. *Neuroscience* **118**, 577–583.

Kapadia R., Yi J. H. and Vemuganti R. (2008) Mechanisms of anti-inflammatory and neuroprotective actions of PPAR-gamma agonists. *Front Biosci.* **13**, 1813–1826.

Khachaturian A. S., Zandi P. P., Lyketsos C. G. *et al.* (2006) Antihypertensive medication use and incident Alzheimer disease: the Cache County Study. *Arch. Neurol.* **63**, 686–692.

Kirischuk S. and Verkhratsky A. (1996) [Ca2+]i recordings from neural cells in acutely isolated cerebellar slices employing differential loading of the membrane-permeant form of the calcium indicator fura-2. *Pflugers Arch.* **431**, 977–983.

Knock G. A., Mishra S. K. and Aaronson P. I. (1999) Differential effects of insulin-sensitizers troglitazone and rosiglitazone on ion currents in rat vascular myocytes. *Eur. J. Pharmacol.* **368**, 103–109.

Kowalska M. and Disterhoft J. F. (1994) Relation of nimodipine dose and serum concentration to learning enhancement in aging rabbits. *Exp. Neurol.* **127**, 159–166.

Kruglikov I., Gryshchenko O., Shutov L., Kostyuk E., Kostyuk P. and Voitenko N. (2004) Diabetes-induced abnormalities in ER calcium mobilization in primary and secondary nociceptive neurons. *Pflugers Arch.* **448**, 395–401.

Kumar P., Kaundal R. K., More S. and Sharma S. S. (2009) Beneficial effects of pioglitazone on cognitive impairment in MPTP model of Parkinson's disease. *Behav. Brain Res.* **197**, 398–403.

LaFerla F. M. (2002) Calcium dyshomeostasis and intracellular signalling in Alzheimer's disease. *Nat. Rev. Neurosci.* **3**, 862–872.

Lannert H. and Hoyer S. (1998) Intracerebroventricular administration of streptozotocin causes long-term diminutions in learning and memory abilities and in cerebral energy metabolism in adult rats. *Behav. Neurosci.* **112**, 1199–1208.

Launer L. J. (2005) Diabetes and brain aging: epidemiologic evidence. *Curr. Diab. Rep.* **5**, 59–63.

Lee G., Elwood F., McNally J. *et al.* (2002) T0070907, a selective ligand for peroxisome proliferator-activated receptor gamma, functions as an antagonist of biochemical and cellular activities. *J. Biol. Chem.* **277**, 19649–19657.

Levy D. I. and Lipton S. A. (1990) Comparison of delayed administration of competitive and uncompetitive antagonists in preventing NMDA receptor-mediated neuronal death. *Neurology* **40**, 852–855.

Li L. and Holscher C. (2007) Common pathological processes in Alzheimer disease and type 2 diabetes: a review. *Brain Res. Rev.* **56**, 384–402.

Li H. and Wei Q. (2001) Conformation changes in brain calcineurin in diabetic rats with or without treatment with vanadyl sulfate. *IUBMB Life* **51**, 373–376.

Lichtor T., Spagnolo A., Glick R. P. and Feinstein D. L. (2008) PPAR-gamma thiazolidinedione agonists and immunotherapy in the treatment of brain tumors. *PPAR Res.* **2008**, 547470.

Lipton S. A. (2004) Failures and successes of NMDA receptor antagonists: molecular basis for the use of open-channel blockers like memantine in the treatment of acute and chronic neurologic insults. *NeuroRx* **1**, 101–110.

Lipton S. A. and Rosenberg P. A. (1994) Excitatory amino acids as a final common pathway for neurologic disorders. *N. Engl. J. Med.* **330**, 613–622.

Luo Y., Yin W., Signore A. P., Zhang F., Hong Z., Wang S., Graham S. H. and Chen J. (2006) Neuroprotection against focal ischemic brain injury by the peroxisome proliferator-activated receptor-gamma agonist rosiglitazone. *J. Neurochem.* **97**, 435–448.

Maeshiba Y., Kiyota Y., Yamashita K., Yoshimura Y., Motohashi M. and Tanayama S. (1997) Disposition of the new antidiabetic agent pioglitazone in rats, dogs, and monkeys. *Arzneimittelforschung* **47**, 29–35.

Martin G., Schoonjans K., Lefebvre A. M., Staels B. and Auwerx J. (1997) Coordinate regulation of the expression of the fatty acid transport protein and acyl-CoA synthetase genes by PPARalpha and PPARgamma activators. *J. Biol. Chem.* **272**, 28210–28217.

Mattson M. P. and Guo Q. (1997) Cell and molecular neurobiology of presenilins: a role for the endoplasmic reticulum in the pathogenesis of Alzheimer's disease? *J. Neurosci. Res.* **50**, 505–513.

Mattson M. P., Wang H. and Michaelis E. K. (1991) Developmental expression, compartmentalization, and possible role in excitotoxicity of a putative NMDA receptor protein in cultured hippocampal neurons. *Brain Res.* **565**, 94–108.

McNay E. C. (2005) The impact of recurrent hypoglycemia on cognitive function in aging. *Neurobiol. Aging* **26**(Suppl 1), 76–79.

de la Monte S. M., Tong M., Lester-Coll N., Plater M. Jr and Wands J. R. (2006) Therapeutic rescue of neurodegeneration in experimental type 3 diabetes: relevance to Alzheimer's disease. *J. Alzheimer's Dis.* **10**, 89–109.

Moyer J. R. Jr, Thompson L. T., Black J. P. and Disterhoft J. F. (1992) Nimodipine increases excitability of rabbit CA1 pyramidal neurons in an age- and concentration-dependent manner. *J. Neurophysiol.* **68**, 2100–2109.

Moyer J. R. Jr, Power J. M., Thompson L. T. and Disterhoft J. F. (2000) Increased excitability of aged rabbit CA1 neurons after trace eyeblink conditioning. *J. Neurosci.* **20**, 5476–5482.

Munshi M., Grande L., Hayes M., Ayres D., Suhl E., Capelson R., Lin S., Milberg W. and Weinger K. (2006) Cognitive dysfunction is associated with poor diabetes control in older adults. *Diabetes Care* **29**, 1794–1799.

Murchison D., Zawieja D. C. and Griffith W. H. (2004) Reduced mitochondrial buffering of voltage-gated calcium influx in aged rat basal forebrain neurons. *Cell Calcium* **36**, 61–75.

Murphy G. G., Shah V., Hell J. W. and Silva A. J. (2006) Investigation of age-related cognitive decline using mice as a model system: neurophysiological correlates. *Am. J. Geriatr. Psychiatry* **14**, 1012–1021.

Nolte R. T., Wisely G. B., Westin S. *et al.* (1998) Ligand binding and co-activator assembly of the peroxisome proliferator-activated receptor-gamma. *Nature* **395**, 137–143.

Norris J. D., Paige L. A., Christensen D. J., Chang C. Y., Huacani M. R., Fan D., Hamilton P. T., Fowlkes D. M. and McDonnell D. P. (1999) Peptide antagonists of the human estrogen receptor. *Science* **285**, 744–746.

Olney J. W. (2002) New insights and new issues in developmental neurotoxicology. *Neurotoxicology* **23**, 659–668.

Ott A., Stolk R. P., van Harskamp F., Pols H. A., Hofman A. and Breteler M. M. (1999) Diabetes mellitus and the risk of dementia: the Rotterdam Study. *Neurology* **53**, 1937–1942.

Paige L. A., Christensen D. J., Gron H. *et al.* (1999) Estrogen receptor (ER) modulators each induce distinct conformational changes in ER alpha and ER beta. *Proc. Natl Acad. Sci. USA*, **96**, 3999–4004.

Pathan A. R., Viswanad B., Sonkusare S. K. and Ramarao P. (2006) Chronic administration of pioglitazone attenuates intracerebroventricular streptozotocin induced-memory impairment in rats. *Life Sci.* **79**, 2209–2216.

Pedersen W. A. and Flynn E. R. (2004) Insulin resistance contributes to aberrant stress responses in the Tg2576 mouse model of Alzheimer's disease. *Neurobiol. Dis.* **17**, 500–506.

Pedersen W. A., McMillan P. J., Kulstad J. J., Leverenz J. B., Craft S. and Haynatzki G. R. (2006) Rosiglitazone attenuates learning and memory deficits in Tg2576 Alzheimer mice. *Exp. Neurol.* **199**, 265–273.

Porter N. M., Thibault O., Thibault V., Chen K. C. and Landfield P. W. (1997) Calcium channel density and hippocampal cell death with age in long-term culture. *J. Neurosci.* **17**, 5629–5639.

Rangwala S. M. and Lazar M. A. (2002) The dawn of the SPPARMs? *Sci. STKE* **2002**, PE9.

Reagan L. P. (2007) Insulin signaling effects on memory and mood. *Curr. Opin. Pharmacol.* **7**, 633–637.

Reisberg B., Doody R., Stoffler A., Schmitt F., Ferris S. and Mobius H. J. (2003) Memantine in moderate-to-severe Alzheimer's disease. *N. Engl. J. Med.* **348**, 1333–1341.

Riggs B. L. and Hartmann L. C. (2003) Selective estrogen-receptor modulators – mechanisms of action and application to clinical practice. *N. Engl. J. Med.* **348**, 618–629.

Risner M. E., Saunders A. M., Altman J. F., Ormandy G. C., Craft S., Foley I. M., Zvartau-Hind M. E., Hosford D. A. and Roses A. D. (2006) Efficacy of rosiglitazone in a genetically defined population with mild-to-moderate Alzheimer's disease. *Pharmacogenomics J.* **6**, 246–254.

Romera C., Hurtado O., Mallolas J. *et al.* (2007) Ischemic preconditioning reveals that GLT1/EAAT2 glutamate transporter is a novel PPARgamma target gene involved in neuroprotection. *J. Cereb. Blood Flow Metab.* **27**, 1327–1338.

Ryan C. M., Freed M. I., Rood J. A., Cobitz A. R., Waterhouse B. R. and Strachan M. W. (2006) Improving metabolic control leads to better working memory in adults with type 2 diabetes. *Diabetes Care* **29**, 345–351.

Schnaider Beeri M., Goldbourt U., Silverman J. M., Noy S., Schmeidler J., Ravona-Springer R., Sverdlick A. and Davidson M. (2004) Diabetes mellitus in midlife and the risk of dementia three decades later. *Neurology* **63**, 1902–1907.

Schoonjans K., Peinado-Onsurbe J., Lefebvre A. M., Heyman R. A., Briggs M., Deeb S., Staels B. and Auwerx J. (1996) PPARalpha and PPARgamma activators direct a distinct tissue-specific transcriptional response via a PPRE in the lipoprotein lipase gene. *EMBO J.* **15**, 5336–5348.

Steen E., Terry B. M., Rivera E. J., Cannon J. L., Neely T. R., Tavares R., Xu X. J., Wands J. R. and de la Monte S. M. (2005) Impaired insulin and insulin-like growth factor expression and signaling mechanisms in Alzheimer's disease–is this type 3 diabetes? *J. Alzheimer's Dis.* **7**, 63–80.

Strum J. C., Shehee R., Virley D. *et al.* (2007) Rosiglitazone induces mitochondrial biogenesis in mouse brain. *J. Alzheimer's Dis.* **11**, 45–51.

Stutzmann G. E., Smith I., Caccamo A., Oddo S., Parker I. and Laferla F. (2007) Enhanced ryanodine-mediated calcium release in mutant PS1-expressing Alzheimer's mouse models. *Ann. N Y Acad. Sci.* **1097**, 265–277.

Sundararajan S., Jiang Q., Heneka M. and Landreth G. (2006) PPAR-gamma as a therapeutic target in central nervous system diseases. *Neurochem. Int.* **49**, 136–144.

Thibault O. and Landfield P. W. (1996) Increase in single L-type calcium channels in hippocampal neurons during aging. *Science* **272**, 1017–1020.

Thibault O., Hadley R. and Landfield P. W. (2001) Elevated postsynaptic [Ca2+]i and L-type calcium channel activity in aged hippocampal neurons: relationship to impaired synaptic plasticity. *J. Neurosci.* **21**, 9744–9756.

Thoennes S. R., Tate P. L., Price T. M. and Kilgore M. W. (2000) Differential transcriptional activation of peroxisome proliferator-activated receptor gamma by omega-3 and omega-6 fatty acids in MCF-7 cells. *Mol. Cell. Endocrinol.* **160**, 67–73.

Tombaugh G. C., Rowe W. B. and Rose G. M. (2005) The slow after-hyperpolarization in hippocampal CA1 neurons covaries with spatial learning ability in aged Fisher 344 rats. *J. Neurosci.* **25**, 2609–2616.

Trompet S., Westendorp R. G., Kamper A. M. and de Craen A. J. (2008) Use of calcium antagonists and cognitive decline in old age. The Leiden 85-plus study. *Neurobiol. Aging* **29**, 306–308.

Uryu S., Harada J., Hisamoto M. and Oda T. (2002) Troglitazone inhibits both post-glutamate neurotoxicity and low-potassium-induced apoptosis in cerebellar granule neurons. *Brain Res.* **924**, 229–236.

Watson G. S. and Craft S. (2003) The role of insulin resistance in the pathogenesis of Alzheimer's disease: implications for treatment. *CNS Drugs* **17**, 27–45.

Watson G. S., Cholerton B. A., Reger M. A. *et al.* (2005) Preserved cognition in patients with early Alzheimer disease and amnestic mild cognitive impairment during treatment with rosiglitazone: a preliminary study. *Am. J. Geriatr. Psychiatry* **13**, 950–958.

Willson T. M., Cobb J. E., Cowan D. J. *et al.* (1996) The structure-activity relationship between peroxisome proliferator-activated receptor gamma agonism and the antihyperglycemic activity of thiazolidinediones. *J. Med. Chem.* **39**, 665–668.

Xing B., Xin T., Hunter R. L. and Bing G. (2008) Pioglitazone inhibition of lipopolysaccharide-induced nitric oxide synthase is associated with altered activity of p38 MAP kinase and PI3K/Akt. *J. Neuroinflammation* **5**, 4.

Yaffe K., Blackwell T., Kanaya A. M., Davidowitz N., Barrett-Connor E. and Krueger K. (2004) Diabetes, impaired fasting glucose, and development of cognitive impairment in older women. *Neurology* **63**, 658–663.

Yan Q., Zhang J., Liu H., Babu-Khan S., Vassar R., Biere A. L., Citron M. and Landreth G. (2003) Anti-inflammatory drug therapy alters beta-amyloid processing and deposition in an animal model of Alzheimer's disease. *J. Neurosci.* **23**, 7504–7509.

Zhang F., Lavan B. E. and Gregoire F. M. (2007) Selective modulators of PPAR-gamma activity: molecular aspects related to obesity and side-effects. *PPAR Res.* **2007**, 32696.

Zhao X., Ou Z., Grotta J. C., Waxham N. and Aronowski J. (2006) Peroxisome-proliferator-activated receptor-gamma (PPARgamma) activation protects neurons from NMDA excitotoxicity. *Brain Res.* **1073–1074**, 460–469.

Zhou M. and Baudry M. (2006) Developmental changes in NMDA neurotoxicity reflect developmental changes in subunit composition of NMDA receptors. *J. Neurosci.* **26**, 2956–2963.

